Ultrafast activation of the double-exchange interaction in antiferromagnetic manganites

Hortensius, J. R.; Afanasiev, D.; Vistoli, L.; Matthiesen, M.; Bibes, M.; Caviglia, A. D.

DOI
10.1063/5.0156400

Publication date
2023

Document Version
Final published version

Published in
APL Materials

APL Materials

RESEARCH ARTICLE | JULY 07 2023

Ultrafast activation of the double-exchange interaction in antiferromagnetic manganites

Special Collection: Emerging Materials in Antiferromagnetic Spintronics

J. R. Hortensius ; D. Afanasiev ; L. Vistoli ; M. Matthiesen ; M. Bibes ; A. D. Caviglia

APL Mater 11, 071107 (2023)
https://doi.org/10.1063/5.0156400

Ultrafast activation of the double-exchange interaction in antiferromagnetic manganites

Cite as: APL Mater. 11, 071107 (2023); doi: 10.1063/5.0156400
Submitted: 29 April 2023 • Accepted: 19 June 2023 •
Published Online: 7 July 2023

J. R. Hortensius,[1] D. Afanasiev,[2,a)] L. Vistoli,[3] M. Matthiesen,[1] M. Bibes,[3] and A. D. Caviglia[4]

AFFILIATIONS

[1] Kavli Institute of Nanoscience, Delft University of Technology, P.O. Box 5046, 2600 GA Delft, Netherlands
[2] Radboud University, Institute for Molecules and Materials, 6525 AJ Nijmegen, Netherlands
[3] Unité Mixte de Physique, CNRS, Thales, Université Paris-Sud, Université Paris-Saclay, Palaiseau, France
[4] Department of Quantum Matter Physics, University of Geneva, 24, Quai Ernest-Ansermet, CH-1211 Geneva, Switzerland

Note: This paper is part of the Special Topic on Emerging Materials in Antiferromagnetic Spintronics.
[a)] **Author to whom correspondence should be addressed:** d.afanasiev@science.ru.nl

ABSTRACT

In doped manganite systems, strong electronic correlations result in rich phase diagrams where electron delocalization strongly affects the magnetic order. Here, we employ a femtosecond all-optical pump-probe scheme to impulsively photodope the antiferromagnetic parent manganite system $CaMnO_3$ and unveil the formation dynamics of a long-range ferromagnetic state. We resonantly target intense charge transfer electronic transitions in $CaMnO_3$ to photodope the system and probe the subsequent dynamics of both charges and spins using a unique combination of time-resolved terahertz spectroscopy and time-resolved magneto-optical Faraday measurements. We demonstrate that photodoping promotes a long-lived population of delocalized electrons and induces a net magnetization, effectively promoting ferromagnetism resulting from light-induced carrier-mediated short-range double-exchange interactions. The picosecond set time of the magnetization, much longer than the electron timescale, and the presence of an excitation threshold are consistent with the formation of ferromagnetic patches in an antiferromagnetic background.

INTRODUCTION

The strong coupling between charge, spin, and orbital order in the perovskite manganites results in rich phase diagrams[1] and provides fertile ground for phase control experiments at thermodynamic equilibrium through electric fields,[2,3] strain effects,[4] and chemical doping.[5] An emerging approach to control the material phase out of equilibrium is photoexcitation using ultrashort pulses of light. The seminal works of Refs. 6 and 7 demonstrated that photoexcitation with ultrashort laser pulses can trigger an insulator-to-metal transition in the charge-ordered state of antiferromagnetic $Pr_{0.7}Ca_{0.3}MnO_3$. Owing to the strong correlations, the light excitation affects not only the charge degree of freedom but also orbitals and spins, all on sub-picosecond timescales. Indeed, this discovery inspired many studies on the effects of photodoping on the orbital and magnetic order of correlated manganite systems on timescales down to a picosecond.[8–13] Manipulation of the magnetic order has been extensively studied in manganite systems in which the ultrafast emergence of a net magnetization or metallic state after photoexcitation coincides with the melting of charge and orbital order present in the system's ground state.[8–13] In a system where charge and orbital order are absent in the ground state, the photo-excited electrons are the only charge carriers experiencing the double-exchange interaction in the photoinduced transient state. This allows one to decouple and rule out some strong correlation effects as the driving force for the emergence of net magnetization and to study the intrinsic magnetic timescales.

Here, we investigate $CaMnO_3$ [see Fig. 1(a)], the single-valence (Mn^{4+}, d^3) end member of the $La_{1-x}Ca_xMnO_3$ series—the mixed-valence oxides well known for their colossal magnetoresistance.[14] With half-filled t_{2g} orbitals and empty e_g states, the insulating behavior and antiferromagnetism (AFM) of $CaMnO_3$ are the result of strong on-site Coulomb repulsion. Minute electron doping in $CaMnO_3$ results in a transition to a metallic state accompanied by

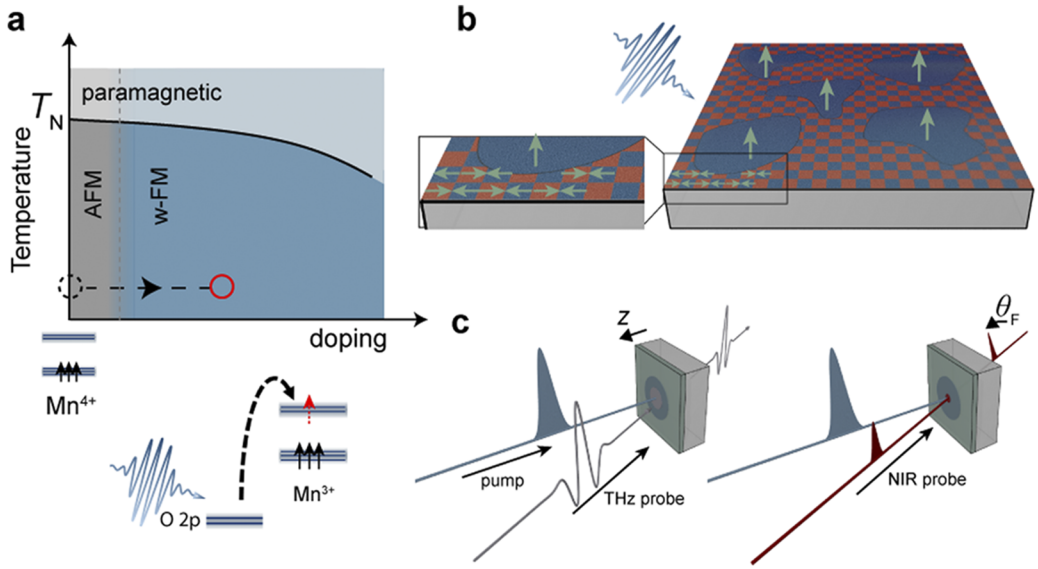

FIG. 1. Ultrafast photodoping of $CaMnO_3$ thin films. (a) (top) Schematic phase diagram of electron-doped $CaMnO_3$. Upon electron doping, the material becomes metallic and weakly ferromagnetic (w-FM). (bottom) A tunable ultrashort pulse excites charge-transfer transitions between the oxygen and Mn-ions. (b) The single valence Mn^{4+} (d^3) spins in $CaMnO_3$ are ordered antiferromagnetically in-plane. Upon chemical or ultrafast electron doping, a macroscopic net magnetic moment emerges in the z-direction. The net magnetic moment is either the result of homogeneous spin canting or ferromagnetic droplets in a collinear AFM background (shown). (c) Schematic of the experiment: The tunable ultrashort pulse (blue) excites an ultrathin CMO film on $YAlO_3$ (001). The induced electron and magnetic dynamics are measured by THz pulses (gray, left) and polarization rotation (θ_F) and transmission changes of the NIR probe pulse (red, right), respectively.

the emergence of ferromagnetic correlations and a net magnetization $\boldsymbol{M}$. The microscopic cause of ferromagnetism is the double-exchange interaction between the mixed-valence manganese ions, Mn^{3+} and Mn^{4+}, which competes with the superexchange interaction and facilitates electron hopping.[15] Yet, the emergence of net magnetization can have different origins. Electron doping of $CaMnO_3$ with just a few percent of tetravalent Ce ions results in metallicity and a progressive increase of the spin canting angle φ to more than 10°,[15,16] giving rise to a sizable net magnetization along the crystallographic z-direction. In contrast, isolated ferromagnetic clusters embedded in an AFM matrix have been argued to be responsible for the macroscopic net magnetic moment in trivalent La-doped $CaMnO_3$[17,18] and Y-doped $CaMnO_3$.[19] These two scenarios, (i) a homogeneously canted AFM state and (ii) phase segregation into regions with collinear antiferromagnetic order and ferromagnetic clusters, are clearly distinct.[20] The distinction raises the intriguing question of the dominant mechanism enabling ultrafast photo-induced dynamics: homogeneous spin canting or inhomogeneous phase segregation.

In this experiment, we target highly absorbing charge-transfer transitions between the oxygen and manganese ions [see Fig. 1(b)] in an epitaxial thin film of $CaMnO_3$. We show that this photodoping introduces delocalized electrons, leading to the emergence of a nonthermal magnetization on picosecond timescales. We also reveal the critical number of photons required to observe this collective response. We discuss the possible contributions of both homogeneous (i.e., coherent) and inhomogeneous (i.e., incoherent) scenarios to the ultrafast magnetization and argue that the ultrafast photodoping results in inhomogeneous phase-segregated magnetization [see Fig. 1(b)].

EXPERIMENT

Compressively strained, 100 nm thick films of $CaMnO_3$ (CMO) were grown on a $YAlO_3$ (YAO) substrate using pulsed laser deposition (details in Ref. 21). Undoped bulk CMO adopts an orthorhombic perovskite *Pbmn* crystal structure. The superexchange interaction between neighboring Mn^{4+} ions gives rise to an antiferromagnetic (AFM) ground state below the Néel temperature T_N of about 120 K. The fundamental absorption edge is independent of the magnetic ordering and is located around an energy of 1.3–1.5 eV.[22] Microscopically, it corresponds to the onset of the strongly absorbing charge-transfer transitions from the O-2p orbitals to the empty Mn-e_g states.[23–25] The YAO substrate is a wide bandgap insulator with negligible absorption below 5 eV,[26] which ensures a negligible contribution to the measured transient response.

Ultrashort (~100 fs) pulses of light are used to resonantly excite the charge-transfer transitions. The excitation pulses are generated by using both the direct and frequency-doubled outputs of an optical parametric amplifier (OPA) operating in the infrared spectral range. This enables a tunable excitation pulse in a large energy range of 0.8–2.5 eV (wavelength λ = 500–1600 nm) across the onset of the Mn–O charge-transfer transitions. We used terahertz (THz) time domain spectroscopy [see Fig. 1(c) and supplementary material, Fig. 1] to measure pump-induced changes in the material's

THz (meV) optical conductivity. To characterize the effect of the photoexcitation on the magnetic order, we additionally measured the pump-induced changes in the transmission and polarization rotation θ of a co-propagating time-delayed, linearly polarized weak probe pulse at 1.55 eV transmitted through the sample [see Fig. 1(c)]. The rotation of this near-infrared (NIR) light is related to the out-of-plane magnetization $\boldsymbol{M}$ due to the magneto-optical Faraday effect, such that $\theta \propto \boldsymbol{M}$.

RESULTS AND DISCUSSION

Photodoping at an excitation energy of 1.94 eV has a pronounced effect on the amplitude of a THz pulse transmitted through the $CaMnO_3$ film [see inset Fig. 2(a)]. Figure 2(a) shows the pump-induced change in the peak value of the transmitted THz pulse as a function of the pump-THz probe delay time. A reduction in the field strength of almost 10% occurs within the first picosecond, which then remains diminished for hundreds of picoseconds. The reduction in the THz amplitude is likely due to increased screening by photoexcited free carriers. The long-lived screening signifies a metallic state persisting beyond carrier lifetimes, which is not uncommon for photo-induced metallic states in manganites.[8] To monitor changes to the magnetic state, we also tracked the time-resolved rotation θ of the NIR-probe polarization plane that appears in response to the photodoping [see Fig. 2(b)]. We observe that there exist magnetic field-dependent and field-independent components at all temperatures [see the supplementary material, Fig. 3]. The field-dependent component changes upon switching the magnetic field polarity [see inset Fig. 2(b)]. Throughout this study, we perform the experiments at two fields of opposite polarity $\pm H$ to eliminate non-magnetic contributions to the polarization rotation and consider the difference $\theta_F = \frac{\theta(+H)-\theta(-H)}{2}$ as a measure of the Faraday rotation that emerges in response to the photo-induced magnetization $\Delta\boldsymbol{M}$ along the z-direction.

Our experiment shows that the growth of magnetization occurs for a few picoseconds, after which the signal decays exponentially over a timescale approaching nanoseconds. To describe its evolution, we analyze the data with the following double exponential function:

$$\theta_F(t) = A(1 - e^{-t/\tau_1}) - B(1 - e^{-t/\tau_1})(1 - e^{-t/\tau_2}). \quad (1)$$

The first term describes the emergence of a net magnetic component (ΔM) of amplitude A in the out-of-plane direction on a timescale τ_1 (see Fig. 2). The second term describes the partial decay (amplitude B) of the signal on a timescale τ_2.

Applying a bias magnetic field with a non-zero component in the z-direction is essential because it predefines the direction of $\boldsymbol{M}$ in the photoinduced magnetic state. Figure 3(a) shows the amplitude of the long-lived component of the transient photoinduced polarization rotation θ at a delay time of 25 ps as a function of the applied

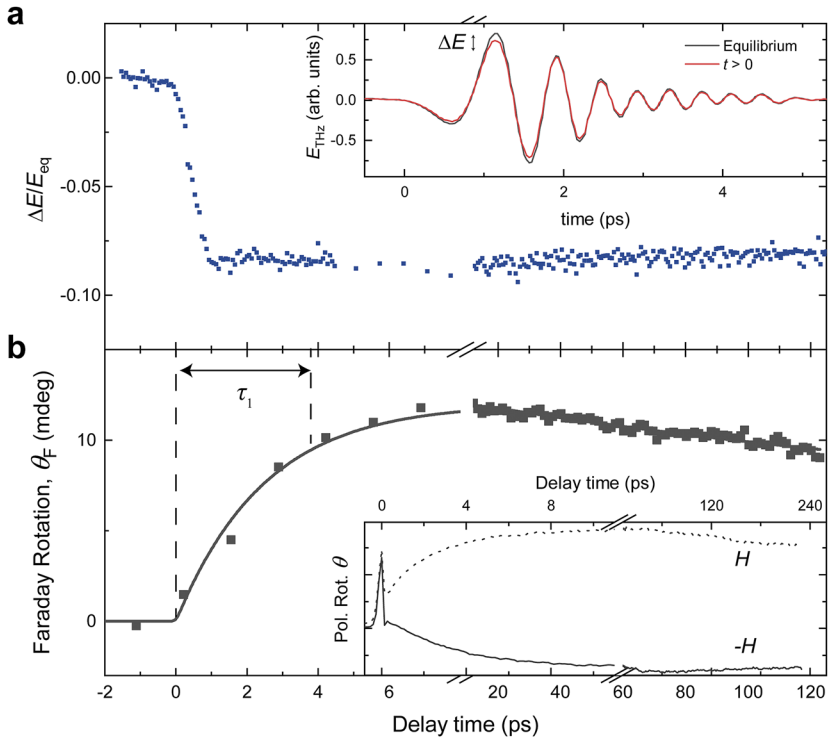

FIG. 2. Ultrafast carrier delocalization and magnetization in $CaMnO_3$. (a) Time-resolved transient change in transmitted THz peak electric field after photodoping (1.94 eV). Inset: Electro-optically detected terahertz transients before (equilibrium) and a few ps after photodoping ($t > 0$). (b) Faraday rotation θ_F probed by [001] polarized NIR pulses after photodoping (1.94 eV). A solid line indicates the fit (see text). Inset: Transient polarization rotation θ for oppositely applied magnetic fields.

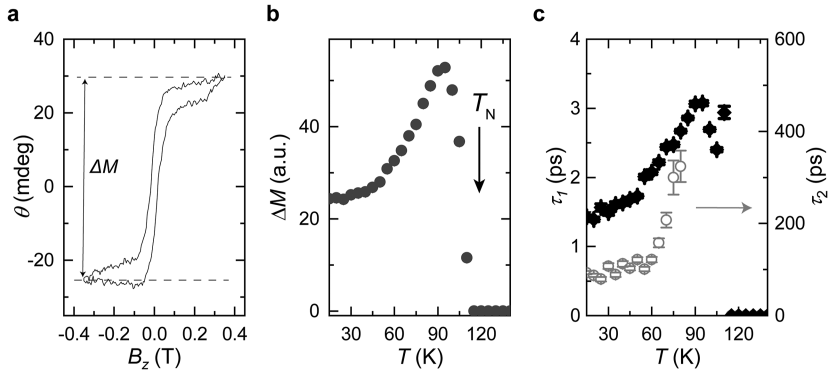

FIG. 3. Characterizing the transient net magnetic moment. (a) Amplitude of the photoinduced polarization rotation at t = 25 ps as a function of the applied magnetic field out-of-plane (T = 105 K). (b) and (c) Amplitude (b) emergence time τ_1 and decay time τ_2 (c) of the induced magnetic component as function of temperature, as extracted with fits Eq. (1) to the time-resolved transient Faraday rotation θ_F ($\pm H$) for different temperatures [see the supplementary material, Fig. 3(a)] after excitation at a photon energy of 1.55 eV.

magnetic field. The data reveal a hysteresis loop and a magnetic remanence in the photoinduced state, indicating that not only the induced magnetic moment but also the equilibrium ground state are susceptible to the magnetic field.

Fitting Eq. (1) to the experimental data (see the supplementary material, Fig. 3), we observe a strong temperature-dependence of the photoinduced magnetization ΔM [see Fig. 3(b)], with a peak around 90 K and a full disappearance of the signal above 110 K. The latter is close to the Néel temperature T_N in the $CaMnO_3$ thin films,[21] another confirmation of the magnetic nature of the measured signal. The non-monotonic temperature dependence can be attributed to the competition between the decrease of both the coercive field and the antiferromagnetic order parameter in the ground state as temperature increases. At low temperatures, the out-of-plane magnetic field used in our experiment (<0.1 T) is not sufficient to overcome the coercive field (up to 1.5 T at low temperatures for 4% Ce-doped samples[21]) and bring the sample into a monodomain state; it thus can only align the net magnetic moment in a part of the domains. The coercive field gets smaller at high temperatures, but simultaneously, the overall AFM order decreases. The latter leads to a reduction of the transient net magnetization ΔM, which is proportional to this AFM order parameter. Note that the lifetime τ_2 of the induced magnetic component also shows a pronounced divergence upon approaching T_N [see Fig. 3(c)], similar to the one observed in photodoping experiments on the strongly correlated antiferromagnetic oxide Sr_2IrO_4.[27]

To understand the microscopic mechanisms underlying these dynamics, we analyze the time τ_1 within which the photoinduced magnetization ΔM grows following the excitation. Our experiments show that this timescale is around 1.5 ps at low temperatures and gradually increases to 3 ps close to the transition temperature [see Fig. 3(c)]. We also note that this time does not depend on the density of photogenerated electrons, as there is no dependence on the pump fluence and pump photon energy (see the supplementary material, Figs. 6 and 7). Interestingly, this time is significantly longer than the pump-induced changes to the conductivity, occurring faster than 0.5 ps [see Fig. 2(a)], indicating a delayed magnetic response. This observation indicates a clear distinction between the electronic and magnetic responses of the material. At the same time, the magnetic response time is still substantially faster than typical spin-lattice relaxation times (~100 ps), which determine the interaction with the lattice—an angular momentum reservoir. We note that similar decoupling has been reported earlier in thin films of the spin glass $Gd_{0.55}Sr_{0.45}MnO_3$.[11]

Measurements at different excitation fluences F reveal the presence of a critical (threshold) fluence F_{th} for the magnetic signal to appear [Fig. 4(a)]. In contrast, there is no threshold present for both the time-resolved THz [see Fig. 4(b)] and NIR-probe (see the supplementary material, Fig. 5) transmission measurements, which represent the pump-induced changes to the electronic system. This indicates that while the number of photoexcited electrons is directly proportional to the light intensity, a pronounced excitation threshold of around 0.004 electrons per manganese ion (0.4% doping) is required to induce a net magnetization.

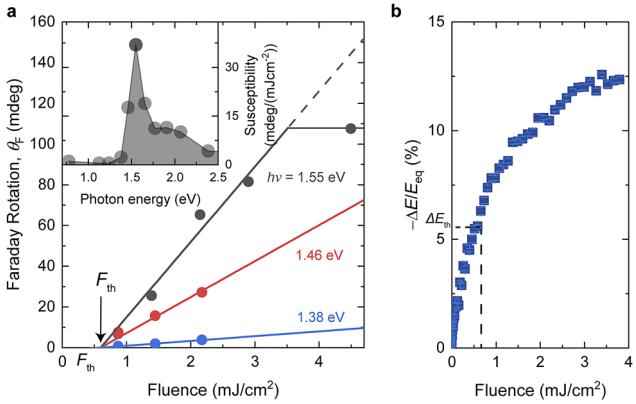

FIG. 4. Photodoping selectivity and threshold. (a) Peak Faraday rotation for different fluences and different excitation photon energies with global linear fits, with shared critical fluence F_{th} for all photon energies. Inset: The resulting susceptibility as a function of the excitation photon energy. (b) Transient (t = 10 ps) change in the THz peak electric field transmitted by the $CaMnO_3$ film after excitation at 1.94 eV.

Before outlining this process, we try to understand the relation between photon energy and the induced magnetic moment by scanning the photon energy across the edge of the charge-transfer transitions. Measurements at different fluences enable the extraction of a photo-susceptibility [see Fig. 4(a)]—the ratio between the induced magnetic component and the fluence used in the experiments. In the inset of Fig. 4(a), we show this extracted quantity for different photon excitation energies within the charge transfer absorption line. The data show a rapid increase in susceptibility around 1.5 eV, corresponding to the onset of the charge-transfer bandgap in $CaMnO_3$.[24] The absence of a sizable signal at photon energies below the material's bandgap supports the proposed microscopic origin of photoinduced magnetization. The decrease of the signal at higher energies can be the result of a penetration depth mismatch due to the difference in photon energy between the excitation and probing light (1.55 eV) or might be caused by enhanced absorption resulting in a thermal quenching of the antiferromagnetic spin order. The changes in the transient NIR transmission show a similar onset close to 1.5 eV, which, in contrast, does not reduce as strongly at higher photon energies (see the supplementary material, Fig. 5), another example of the different electronic (transmission) and magnetic responses to the photoexcitation.

The emergence of an equilibrium net magnetization in doped $CaMnO_3$, driven by the double-exchange interaction, can proceed in two different ways: (i) in a "coherent" form, with electron-doping leading to homogeneous canting of the antiferromagnetic sublattices (as in Ce-doped $CaMnO_3$), or (ii) in a phase separated form in which ferromagnetic droplets appear in an antiferromagnetic background (as in La-doped and Y-doped $CaMnO_3$). In the first scenario, we expect an instantaneous, coherent response after photodoping. In contrast, our experiments indicate that the transient net magnetic moment appears to arise on a relatively slow timescale, which supports the second scenario of ferromagnetic droplets. In addition, we also observe an excitation threshold for the net magnetization to appear, absent in the case of the electronic response (THz transmission measurements). As the applied magnetic field biases the direction of the emerging magnetic moment of the conducting droplets, the lack of a net macroscopic magnetization below the threshold indicates that for low excitation fluences, the droplets are below a critical size and cannot develop a magnetic moment. The mere presence of delocalized electrons is not sufficient, as a minimum density and size of these droplets are required for them to interact and form a macroscopic magnetization. The threshold also indicates the presence of a metastable nonequilibrium state associated with net magnetization and thus may support an inhomogeneous scenario characterized by phase coexistence. Therefore, the observation of an excitation threshold supports the scenario of a transient phase-separated state, where photoexcitation leads to patches of the ferromagnetic phase emerging in the antiferromagnetic background. In this scenario, the minimum fluence corresponds to the percolation threshold of ferromagnetic clusters required to establish long-range macroscopic magnetic order. As the change in THz transmission at the threshold fluence amounts to roughly 40% of the saturation value [see Fig. 4(b)], this could indicate a percolation threshold for the magnetic order of 0.4. This is close to the required site filling probability $p = 0.31$ in 3D cubic networks to establish percolation.[28]

In this scenario, the delayed response of the magnetic dynamics can be explained by the mutual alignment of spins between individual droplets. The antiferromagnetic background arguably plays a decisive role in this process, as the photoinduced magnetization appears exclusively below T_N. The alignment is likely to be mediated by the emission of elementary spin-wave excitations—magnons that can propagate and establish spin-spin correlations. Indeed, the strong magneto-crystalline anisotropy inherent to $CaMnO_3$ (and other manganites) thin films[21] causes the lowest frequency magnons to have frequencies in the sub-THz frequency range, corresponding to the observed timescales of several picoseconds.[29]

Finally, to improve our understanding of the transient doping, we compared the photo-induced magnetic component in the $CaMnO_3$ thin film with a lightly (1%) Ce-doped film. These films are intrinsically electron-doped in equilibrium and have a larger canting of the magnetic sublattices, which might affect the light-induced dynamics. While we observe a smaller induced magnetization at all temperatures compared to the $CaMnO_3$ film, the overall time-evolution is very similar (see the supplementary material Fig. 8). This implies that with the present excitation fluences, the slightly altered ground state with a small net magnetic moment does not change the dynamics substantially.

CONCLUSION

In summary, we have investigated the ultrafast response of thin films of the antiferromagnetic manganite parent compound $CaMnO_3$ after photoexcitation of the charge-transfer transition from oxygen to manganese ions. Using time-resolved THz transmission measurements, we probe the presence of a long-lived state with increased THz photoconductivity, indicating carrier delocalization. Through time-resolved Faraday measurements, we observe the emergence of a macroscopic net magnetic component in an otherwise antiferromagnetic compound, the result of activating carrier-mediated double-exchange between the manganese ions. In the absence of any charge- and orbital-ordered electrons in the ground state, the macroscopic ferromagnetic moment is formed in around 2 ps, which we attribute to the typical interaction of the constituting ferromagnetic clusters in the AFM background. The macroscopic moment is characterized by a small excitation threshold of ~0.004 electrons per Mn-ion, which indicates a profound difference with chemical electron doping. Our work contributes to the understanding of ultrafast cooperative phenomena in complex materials where a strong interplay of different degrees of freedom is present. More specifically, we show that the antiferromagnetic manganites demonstrate a remarkable susceptibility to photoexcitation, with ultrafast responses and persistent changes in both magnetic and electric properties. This makes the manganites excellent candidates for ultrafast switching devices, and perhaps they will eventually find application in ultrafast spintronic devices.[30]

SUPPLEMENTARY MATERIAL

See the supplementary material for details on the experimental (THz) setup and additional measurement data.

ACKNOWLEDGMENTS

This research was supported by the EU through the European Research Council, Grant No. 677458 (AlterMateria and QED Materials) and Grant No. 615759 ("MINT"), the Swiss State Secretariat for Education, Research and Innovation (SERI), the Gordon and Betty Moore Foundation, Grant No. GBMF10451 to A.D.C., and the Netherlands Organization for Scientific Research (NWO/OCW) as part of the VENI-VIDI-VICI program.

AUTHOR DECLARATIONS

Conflict of Interest

The authors have no conflicts to disclose.

Author Contributions

J. R. Hortensius: Formal analysis (lead); Investigation (lead); Methodology (equal); Writing – original draft (lead). **D. Afanasiev**: Conceptualization (equal); Formal analysis (equal); Investigation (equal); Methodology (equal); Writing – original draft (equal). **L. Vistoli**: Investigation (supporting); Resources (lead); Writing – review & editing (supporting). **M. Matthiesen**: Formal analysis (supporting); Investigation (supporting); Writing – review & editing (equal). **M. Bibes**: Conceptualization (equal); Funding acquisition (equal); Methodology (equal); Resources (lead); Supervision (equal); Writing – review & editing (equal). **A. D. Caviglia**: Conceptualization (equal); Funding acquisition (equal); Methodology (equal); Supervision (lead); Writing – original draft (equal).

DATA AVAILABILITY

Source data for figures will be made publicly available at Zenodo at 10.5281/zenodo.8034596. All other data that support the findings of this paper are available from the corresponding authors upon request.

REFERENCES

[1]E. Dagotto, T. Hotta, and A. Moreo, "Colossal magnetoresistant materials: The key role of phase separation," Phys. Rep. **344**(1–3), 1–153 (2001).
[2]S. Mathews *et al.*, "Ferroelectric field effect transistor based on epitaxial perovskite heterostructures," Science **276**(5310), 238–240 (1997).
[3]H. Tanaka, J. Zhang, and T. Kawai, "Giant electric field modulation of double exchange ferromagnetism at room temperature in the perovskite manganite/titanate *p–n* junction," Phys. Rev. Lett. **88**(2), 027204 (2002).
[4]Y. Konishi *et al.*, "Orbital-state-mediated phase-control of manganites," J. Phys. Soc. Jpn. **68**(12), 3790–3793 (1999).
[5]H. Y. Hwang *et al.*, "Lattice effects on the magnetoresistance in doped $LaMnO_3$," Phys. Rev. Lett. **75**(5), 914 (1995).
[6]K. Miyano *et al.*, "Photoinduced insulator-to-metal transition in a perovskite manganite," Phys. Rev. Lett. **78**(22), 4257 (1997).
[7]M. Fiebig *et al.*, "Visualization of the local insulator-metal transition in $Pr_{0.7}Ca_{0.3}MnO_3$," Science **280**(5371), 1925–1928 (1998).
[8]N. Takubo *et al.*, "Persistent and reversible all-optical phase control in a manganite thin film," Phys. Rev. Lett. **95**(1), 017404 (2005).
[9]K. Miyasaka *et al.*, "Ultrafast photoinduced magnetic moment in a charge-orbital-ordered antiferromagnetic $Nd_{0.5}Sr_{0.5}MnO_3$ thin film," Phys. Rev. B **74**(1), 012401 (2006).
[10]M. Matsubara *et al.*, "Photoinduced switching between charge and orbital ordered insulator and ferromagnetic metal in perovskite manganites," Phys. Rev. B **77**(9), 094410 (2008).
[11]M. Matsubara *et al.*, "Ultrafast photoinduced insulator-ferromagnet transition in the perovskite manganite $Gd_{0.55}Sr_{0.45}MnO_3$," Phys. Rev. Lett. **99**(20), 207401 (2007).
[12]P. Beaud *et al.*, "Ultrafast structural phase transition driven by photoinduced melting of charge and orbital order," Phys. Rev. Lett. **103**(15), 155702 (2009).
[13]P. C. Lingos *et al.*, "Correlating quasiparticle excitations with quantum femtosecond magnetism in photoexcited nonequilibrium states of insulating antiferromagnetic manganites," Phys. Rev. B **95**(22), 224432 (2017).
[14]S. Jin *et al.*, "Thousandfold change in resistivity in magnetoresistive La-Ca-Mn-O films," Science **264**(5157), 413–415 (1994).
[15]E. a. N. Caspi *et al.*, "Structural and magnetic phase diagram of the two-electron-doped $(Ca_{1-x}Ce_x)MnO_3$ system: Effects of competition among charge, orbital, and spin ordering," Phys. Rev. B **69**(10), 104402 (2004).
[16]H. Ohnishi *et al.*, "Spin-canting in lightly electron-doped $CaMnO_3$," Phys. Rev. B **85**(16), 165128 (2012).
[17]J. J. Neumeier and J. L. Cohn, "Possible signatures of magnetic phase segregation in electron-doped antiferromagnetic $CaMnO_3$," Phys. Rev. B **61**(21), 14319 (2000).
[18]C. D. Ling *et al.*, "Inhomogeneous magnetism in La-doped $CaMnO_3$. I. Mesoscopic phase separation due to lattice-coupled ferromagnetic interactions," Phys. Rev. B **68**(13), 134439 (2003).
[19]N. Sharma *et al.*, "Phase separated behavior in yttrium doped $CaMnO_3$," Mater. Res. Bull. **77**, 284–290 (2016).
[20]D. Khomskii, *Transition Metal Compounds* (Cambridge University Press, 2014).
[21]L. Vistoli *et al.*, "Giant topological Hall effect in correlated oxide thin films," Nat. Phys. **15**(1), 67–72 (2019).
[22]M.-A. Husanu *et al.*, "Electron-polaron dichotomy of charge carriers in perovskite oxides," Commun. Phys. **3**(1), 62 (2020).
[23]J. H. Jung *et al.*, "Determination of electronic band structures of $CaMnO_3$ and $LaMnO_3$ using optical-conductivity analyses," Phys. Rev. B **55**(23), 15489 (1997).
[24]S. Asanuma *et al.*, "Relationship between resistive switching characteristics and band diagrams of Ti/$Pr_{1-x}Ca_xMnO_3$ junctions," Phys. Rev. B **80**(23), 235113 (2009).
[25]M. Sotoudeh *et al.*, "Electronic structure of $Pr_{1-x}Ca_xMnO_3$," Phys. Rev. B **95**(23), 235150 (2017).
[26]S. A. Basun *et al.*, "Optical and photoelectrical studies of charge-transfer processes in $YAlO_3$:Ti crystals," Phys. Rev. B **54**(9), 6141 (1996).
[27]D. Afanasiev *et al.*, "Ultrafast spin dynamics in photodoped spin-orbit Mott insulator Sr_2IrO_4," Phys. Rev. X **9**(2), 021020 (2019).
[28]D. Stauffer and A. Aharony, *Introduction to Percolation Theory*, 2nd ed. (Taylor and Francis, London, 1992), p. 18.
[29]S. Mitsudo *et al.*, "Submillimeter wave ESR measurement of $LaMnO_3$," J. Magn. Magn. Mater. **177–181**, 877–878 (1998).
[30]A. El-Ghazaly *et al.*, "Progress towards ultrafast spintronics applications," J. Magn. Magn. Mater. **502**, 166478 (2020).